

## Changes in hydroclimatic trends in the Kunhar River Watershed

Haseeb Akbar<sup>1,2</sup> and Shabbir H. Gheewala<sup>1,2,\*</sup>

<sup>1</sup>The Joint Graduate School of Energy and Environment, King Mongkut's University of Technology Thonburi, 126 Prachauthit Rd., Bangmod, Tungkru, Bangkok 10140, Thailand

<sup>2</sup>Center of Excellence on Energy Technology and Environment (CEE), PERDO, Ministry of Higher Education, Science, Research and Innovation, Bangkok, Thailand

\*Correspondence; E-Mail: shabbir\_g@jgsee.kmutt.ac.th, Tel.: +66-2470-8309, Fax: +66-2872-9805

**Abstract:** Climate change is one of the major threats to humanity in recent times. It has a significant potential to disturb the water cycle which additionally accelerates many problems i.e. water availability, agriculture yields, damage to the ecosystem, etc. That is why it is important to understand the climatic changes in the rural and agrarian-based basin. Therefore, the focus of this study was to detect the changes in the climatic indices and parameters in the Kunhar river basin, Pakistan. Box and whisker plots, RClimDex tool, Mann Kendall test, and Inverse distance weighted (IDW) were used to observe the basic statistics, variations in the climatic indices, trends of climatic parameters, and their significance and spatial distribution of the climatic parameters respectively, over the Kunhar River basin. For the baseline period (1979-2014), it was found that the maximum and minimum temperatures were increasing significantly. However, precipitation, wind speed, and relative humidity were decreasing significantly. Changes in the climatic parameters were more significant in the lower half of the basin than the upper. Changes in the seasonal flow were more significant than annual. Runoff was increasing at the rate of  $0.415 \text{ m}^3\text{s}^{-1}$  per spring season and decreasing at the rate of  $0.415 \text{ m}^3\text{s}^{-1}$  per summer season, which is a clear indication of peak shift in the backward direction. These changes affect the agriculture yields, water availability, and ecosystem of the basin.

**Keywords:** Hydroclimate, RClimDex, Mann-Kendall, Kunhar.

### 1. Introduction

Climate change plays a key role in the transformation of the hydrological cycle [1]. Hydro-climatic trends have vital importance in the field of water resources. The hydro-climatic system is very complex because it depends upon many factors such as the atmosphere, hydrosphere, cryosphere, geosphere, and biosphere [2]. Change in even any one of these factors may alter the hydrological cycle substantially. For example, the concentration of greenhouse gases (GHGs), especially carbon dioxide, since the mid of the last century, has increased exponentially over the last few decades, resulting in global warming. Anthropogenic forces such as the fossil fuel, land-use changes, and quick industrialization are considered to be the main reasons for the increased GHGs in the atmosphere [3]. Especially in the high mountainous basins, global warming triggers the melting of snow, increase in rainfall rather than snowfall, depletion of glaciers [4], change in evaporation and cloud formation, all of which ultimately altering the hydrological conditions of that region [5] and also increasing the threat of extreme events (flood and drought) around the globe [6]. Investigating the trends of the past hydro-climatic parameters can play a vital role in future impact estimation [7]. All these factors make it more important to the researchers to analyze the trends of hydroclimatic parameters worldwide.

Substantial development had been made in the field of trend analysis in the last few decades [8]. In the lower reaches of the Shiyang River Basin in China, a hydro-climatic analysis carried out through the Mann-Kendall test and wavelet analysis. It revealed a decrease in streamflow, an increase in temperature, and no change in precipitation [2]. Hydro-climatic trend analysis carried out in the Tarim River Basin, China with the help of the Mann-Kendall test showed an increase in mean annual temperature and precipitation while runoff showed mix trends during 1960-2007 [9].

Spatial variation in precipitation was analyzed by using the correlation and regression analysis in the upper Indus basin, Pakistan. A significant positive correlation between the winter North Atlantic Oscillation Index and winter precipitation was observed. However, the opposite relation was observed for summer precipitation at a few stations [10]. Many investigations have been conducted in the two main basins of Pakistan, the Indus basin [11-13], and the Mangla basin [14-15] to attract the attention of the global scientific community towards massive areas. However, in the developing countries, the rural and smaller watersheds have more importance over the larger ones especially when 'sustainability' is considered [16]. The climate change profile of Pakistan was investigated. It was found that the mean annual temperature has risen by  $0.54^\circ\text{C}$  from 1960 to 2013. The rate of increase has been  $0.01^\circ\text{C}$  per year. Moreover, the annual precipitation increased by 61 mm in Pakistan from 1901 to 2007 [17].

Water plays a crucial part in the rural basins like Kunhar basin for socio-economic activities such as agriculture, tourism, fish farming, and hydropower. Kunhar River basin is famous for its mountains [18] and adventure tourism [19], it has many hydropower plants, a few completed, some under construction and many raw sites [20]. It also has a unique location in a country due to valuable dry fruit production. It has a complex topography and a lot of climatic variations across the basin. All these factors make it important to investigate the hydroclimatic trends of time series data of this basin.

Many studies have been conducted to investigate the trends of hydroclimatic parameters in the Kunhar river basin. However, almost all of them used climatic data of two or three stations from the Pakistan Meteorological Department and used the Mann Kendall test. Due to its complex topography and climatic variations, three stations are not enough to represent the true climatic picture of the basin. Until now, no one has used RClimDex along with the Mann Kendall test to investigate the variations in the climatic

parameters and indices. Moreover, climatic data of eight stations from a global data source were used to improve the true representation of the climatic situation of the basin. Therefore, the objectives of this research are to investigate the trends of climatic parameters and indices on the spatial and temporal bases for the baseline period of 1979-2014.

### 1.1 Study Area

The Kunhar watershed spreads between 34.2° to 35.1°N and 73.3° to 74.1°E; area of this watershed is 2632 km<sup>2</sup>. River Kunhar originates from Babosar Top (4173m) near Station 8 (Figure 1) and falls into the River Neelam near Muzaffarabad. The total length of the main reach of the Kunhar River is 171 km. The lowest elevation point of this watershed is 642 m high from the mean sea level and the highest elevation point of the basin is 5106 m from the mean sea level. The average slope of the Kunhar watershed is 53%. There is a two-stream gauge at Naran and Garhi-Habibullah in the River Kunhar. Eight climatic stations were selected across the basin as shown in Figure 1. The Kunhar basin has a variety of vegetation cover as Agricultural Land-Generic, Forest-Deciduous, Pasture, Barren, and Snow [21].

## 2. Materials and Methods

This section describes the data sources and the methods used to accomplish the hydroclimatic analysis required to achieve the goal of this study. The methods used include basic statistics calculations, trend analysis, and spatial distribution analysis via geographical information systems (GIS).

### 2.1. Data Acquisition

Climatic data of one-day temporal resolution for the Kunhar River basin were obtained from the National Centers for Environmental Prediction's Climate Forecast System Reanalysis (CFSR) for 35 (1979-2014) years, its spatial resolution was 30 x 30 km. Six climatic parameters (precipitation, maximum temperature, minimum temperature, wind speed, relative humidity, and solar radiation) were downloaded through the following link; <https://globalweather.tamu.edu/>. Streamflow data for the stations of Naran and Ghari Habibullah/Talhatta were collected by the Surface Water Hydrology Project (SWHP). Temporal resolution is one day and temporal length 67 years from 1961 to 2017. Detail of each station is given in Table 1.

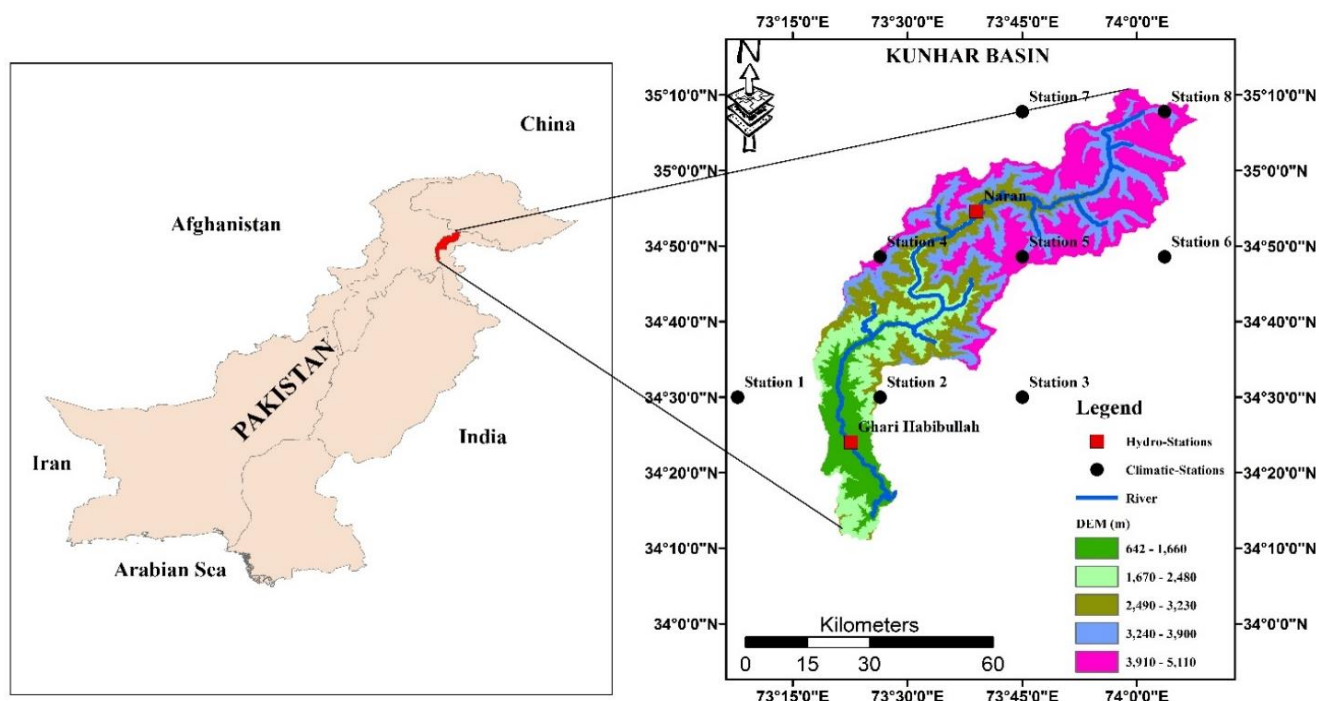


**Figure 1.** Location of the study area, Kunhar River watershed.

**Table 1.** Details of the hydro-climatic stations and available data.

Stations	Longitude	Latitude	Elevation	Tmax	Tmin	PPT <sup>1</sup>	Wind Speed	RH <sup>2</sup>	SR <sup>3</sup>	Runoff
Station 1	73.13	34.5	1367	✓	✓	✓	✓	✓	✓	
Station 2	73.44	34.5	2829	✓	✓	✓	✓	✓	✓	
Station 3	73.75	34.5	3304	✓	✓	✓	✓	✓	✓	
Station 4	73.44	34.81	4316	✓	✓	✓	✓	✓	✓	
Station 5	73.75	34.81	3720	✓	✓	✓	✓	✓	✓	
Station 6	74.06	34.81	4230	✓	✓	✓	✓	✓	✓	
Station 7	73.75	35.13	3284	✓	✓	✓	✓	✓	✓	
Station 8	74.06	35.13	3777	✓	✓	✓	✓	✓	✓	
Naran	73.65	34.91	2409							✓
Garhi Habibullah	73.36	34.44	854							✓

<sup>1</sup>PPT = precipitation, <sup>2</sup>RH = relative humidity, <sup>3</sup>SR = Solar Radiation

**Table 2.** The definitions and units of all the indices.

ID	Indicator name	Definitions	Units
<b>Hot Extremes</b>			
SU25	Summer days	Annual count when Tmax (daily maximum) >25°C	Days
TXx	Max Tmax	Monthly maximum value of daily maximum temp	°C
TNx	Max Tmin	Monthly maximum value of daily minimum temp	°C
TN90p	Warm nights	Percentage of days when Tmin>90th percentile	Days
TX90p	Warm days	Percentage of days when Tmax>90th percentile	Days
WSDI	Warm spell duration indicator	Annual count of days with at least 6 consecutive days when Tmax>90th percentile	Days
<b>Cold Extremes</b>			
FD0	Frost days	Annual count when Tmin (daily minimum) <0°C	Days
TXn	Min Tmax	Monthly minimum value of daily maximum temp	°C
TNn	Min Tmin	Monthly minimum value of daily minimum temp	°C
TN10p	Cool nights	Percentage of days when Tmin<10th percentile	Days
TX10p	Cool days	Percentage of days when Tmax<10th percentile	Days
CSDI	Cold spell duration indicator	Annual count of days with at least 6 consecutive days when Tmin<10th percentile	Days
<b>Precipitation Extremes</b>			
Rx5day	Max 5-day precipitation amount	Monthly maximum consecutive 5-day precipitation	mm
SDII	Simple daily intensity index	Annual total precipitation divided by the number of wet days (defined as PPT>=1.0mm) in the year	mm/day
R10	Number of days above 10 mm	Annual count of days when PPT>=10 mm	Days
R50	Number of days above 50 mm	Annual count of days when PPT>=50 mm, 50 is user defined threshold	Days
CDD	Consecutive dry days	Maximum number of consecutive days with RR<1mm	Days
CWD	Consecutive wet days	Maximum number of consecutive days with RR>=1mm	Days
R95p	Very wet days	Total annual PPT when PPT>95 <sup>th</sup> percentile	mm
R99p	Extremely wet days	Total annual PPT when PPT>99 <sup>th</sup> percentile	mm
Prcptot	Annual total wet-day precipitation	Total annual PPT in wet days (PPT>=1mm)	mm

**2.2 Methodology**

In this study, the hydroclimatic analysis was divided into four sections; basic statistics through box and whisker graphs, trend analysis, climatic extremes, and spatial analysis. All four analyses were carried out by different tools. Details are given in the subsections below.

**2.2.1 Basic Statistics**

Basic statistics (mean, median, quartiles, and ranges) of the hydroclimatic data were simply obtained through box and whisker plots. It gives an easy understanding of basic statistics (mean, median, quartiles, and ranges) of each station and the comparison with others.

**2.2.2 Climatic extremes**

To investigate the climatic extreme indices, the RClimDex tool has extensively been used in many pieces of research [22-24] in the last decade. The RClimDex tool was developed by the Expert Team for Climate Change Detection Monitoring and Indices (ETCCDMI). RClimDex is also used as a screening tool to check the data quality [25], such as negative precipitation, outliers, and minimum temperature higher than maximum. The RClimDex tool is used to determine three types of climatic extremes; hot extremes, cold extremes, and precipitation extremes [26]. The definitions and units of all the indices are presented in Table 2.

**2.2.3 Trend analysis**

Many trend analysis tools are available, which can broadly be categorized into two main types, non-parametric and parametric [11]. Data should be normally distributed and free from outliers for the parametric approach and there is no such compulsion for the non-parametric approach [12, 27]. That is why the Mann-Kendall test is one of the non-parametric approaches most widely used [7, 13]. The Mann Kendall test is a rank-based approach that compares each unique value with remaining values in sequential order [28] as the test statistic (S) is given in Equation 1,

$$S = \sum_{k=1}^{n-1} \sum_{j=k+1}^n Sgn(X_j - X_k) \tag{1}$$

Where Sg indicates the sign of trend either negative or positive, and n the length of the dataset; Sgn combined represents the sign of a complete dataset. X<sub>j</sub> - X<sub>k</sub> are the sequential data values, explained further in Equation 2.

$$Sgn(X_j - X_k) = \begin{cases} 1 & \text{if } (X_j - X_k) > 0 \\ 0 & \text{if } (X_j - X_k) = 0 \\ -1 & \text{if } (X_j - X_k) < 0 \end{cases} \tag{2}$$

For samples >10, the test is conducted using the normal distribution [29] with the expectation (E) as given in Equation 3.

$$E[S] = 0 \tag{3}$$

Variance (Var) as expressed in Equation 4; where t<sub>p</sub> is the number of data points in the p<sup>th</sup> tied group and q is the number of tied groups in the dataset.

$$Var(S) = \frac{1}{18} [n(n-1)(2n+5) - \sum_{p=1}^q t_p(t_p-1)(2t_p+5)] \tag{4}$$

The standardized test statistic (Z<sub>mk</sub>) is calculated as mentioned in Equation 5.

$$Z_{mk} = \begin{cases} \frac{S-1}{\sqrt{Var(S)}} & \text{if } S > 0 \\ \frac{S+1}{\sqrt{Var(S)}} & \text{if } S < 0 \\ 0 & \text{if } S = 0 \end{cases} \tag{5}$$

Where the value of Z<sub>mk</sub> is the Mann Kendall test statistic that follows a standard normal distribution with mean 0 and variance 1. The Z<sub>mk</sub> value can be related to a p-value of a specific trend. The p-value is a measure of evidence against the null hypothesis of no change. The smaller is the p-value, the greater is the strength of the evidence against the null hypothesis. In a 2-sided test for

trend, the null hypothesis of no trend is accepted if  $-Z_{1-\alpha/2} \leq Z_{mk} \leq Z_{1-\alpha/2}$ , where  $\alpha$  is the significance level (Sig.) that indicates the trend strength. In the present study, the trends are categorized as very strong (VS), strong (S), weak (W), little (L) and very little (VL) according to the respective p-values as follows:  $0.0 < p \leq 0.01$  (VS),  $0.01 < p \leq 0.05$  (S),  $0.05 < p \leq 0.10$  (W),  $0.10 < p \leq 0.50$  (L), and  $0.50 < p \leq 1.0$  (VL) [11].

Many researchers [30-31] have estimated the slope of the time series data with the help of Sen's slope method. Its advantage is that it is unresponsive to outliers. In this method, slopes are calculated for every pair of the ordinate time points and then the median of these slopes used as an estimate of the overall slope. [26, 32]. The estimate of the trend the Sen's slope " $Q$ " (change per unit time) is given in Equation 6.

$$Q = \text{median} \left( \frac{X_j - X_k}{j - k} \right) \forall k < j \quad (6)$$

Where;  $X_j$  is the data value at time  $j$ ,  $X_k$  is the data value at time  $k$  and  $j$  is the time after  $k$  ( $j > k$ ).

#### 2.2.4. Spatial distribution analysis

To investigate the spatial distribution of hydroclimatic parameters, Arc GIS was used. Spatial variations in the climatic parameters were determined by interpolating between the climatic stations. The Inverse Distance Weighted (IDW) tool was used for the interpolation of climatic parameters.

### 3. Results and Discussion

In this section, the climatic data from eight different stations are analyzed. Basic statistics of data were examined by box and whisker graph, climatic extremes were analyzed by RClimDex and trend analysis was carried through the Mann-Kendall test. Similarly, streamflow data of two stations were analyzed by the box and whisker graph and Mann Kendall test.

#### 3.1 Box and whisker plots

All the six parameters of climatic data of eight stations and streamflow data of two stations were analyzed through box and whisker plots.

##### 3.1.1 Streamflow

The average annual streamflow of two stations; Naran and Ghari Habibullah was analyzed through box and whisker plots to check the mean and other basic statistics of the runoff of the Kunhar River basin. It was found that the average annual runoff of the Naran and Ghari-Habibullah stations was  $47 \text{ m}^3/\text{s}$  and  $102 \text{ m}^3/\text{s}$  respectively. In the period 1961-2017. Moreover, the highest flows at Naran and Ghari-Habibullah were detected as  $63 \text{ m}^3/\text{s}$  and  $155 \text{ m}^3/\text{s}$ . Similarly, the lowest runoffs at Naran and Ghari-

Habibullah were detected as  $30 \text{ m}^3/\text{s}$  and  $54 \text{ m}^3/\text{s}$  respectively. Graphical representation of the average annual streamflow in the form of box and whisker plot is shown in Figure 2. A hydroclimatic study was conducted for the Jhelum River basin. It discussed almost similar results of streamflow at Naran and Ghari Habibullah stations [3, 14].

#### 3.1.2 Temperature

The Kunhar river basin has only  $2632 \text{ km}^2$  area, but the variations in climatic parameters from top to bottom are vast due to its complex topography. Both minimum and maximum average annual temperatures were higher at low altitude areas. The maximum and minimum temperatures in the Kunhar basin decreased with increasing altitude. Station 1 is situated at the downstream side of the Kunhar River and its average annual maximum and minimum temperatures were  $21.75^\circ\text{C}$  and  $9.26^\circ\text{C}$  respectively. On the other hand, Station 8 had an average annual maximum and minimum temperatures of  $4.68^\circ\text{C}$  and  $-5.50^\circ\text{C}$  correspondingly. Absolute values of the average annual maximum and minimum temperatures at all the stations are given in Figures 3(a) and (b) respectively.

#### 3.1.3 Precipitation

Average annual precipitation in the Kunhar River basin had the lowest value of  $809 \text{ mm}/\text{year}$  at the Station 1 and it increased progressively up to the Station 5, where the precipitation received per annum was  $2651 \text{ mm}$ , which is the highest amount of precipitation per annum received by any station in the Kunhar River basin. Distribution of average annual and some other basic statistics (ranges, quartiles, and outliers) of precipitation over the Kunhar basin is shown in Figure 3(c) for the eight different stations.

#### 3.1.4 Wind Speed

Wind speed plays an important part in the snow accumulated basin in snow hydrology [33]. In the Kunhar River basin, the average annual wind speed was higher at the low altitude stations than the higher ones. The difference between average annual wind speed from upstream to downstream was  $1.24 \text{ m/s}$ . The highest observed average annual wind speed was  $3.71 \text{ m/s}$  at Station 1 and the lowest was  $2.47 \text{ m/s}$  at Station 8. The annual wind speed of all eight stations is given in Figure 3(d).

#### 3.1.5 Relative Humidity

The average annual relative humidity in the Kunhar River basin followed almost the same pattern as precipitation. The lowest average annual relative humidity was  $0.49$  at Station 1, whereas the highest was  $0.81$  at Station 6. However, the value of the average annual relative humidity was almost similar at Stations 5, 6, 7, and 8. The unit of the relative humidity is a fraction in this study. The average annual relative humidity at all stations is given in Figure 3(e).

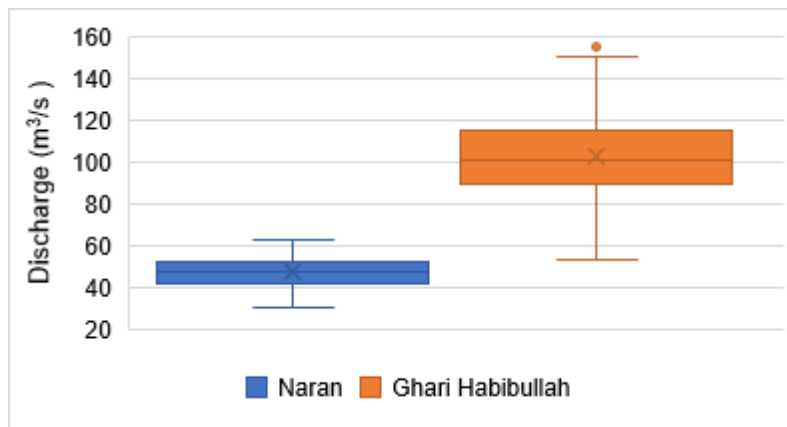
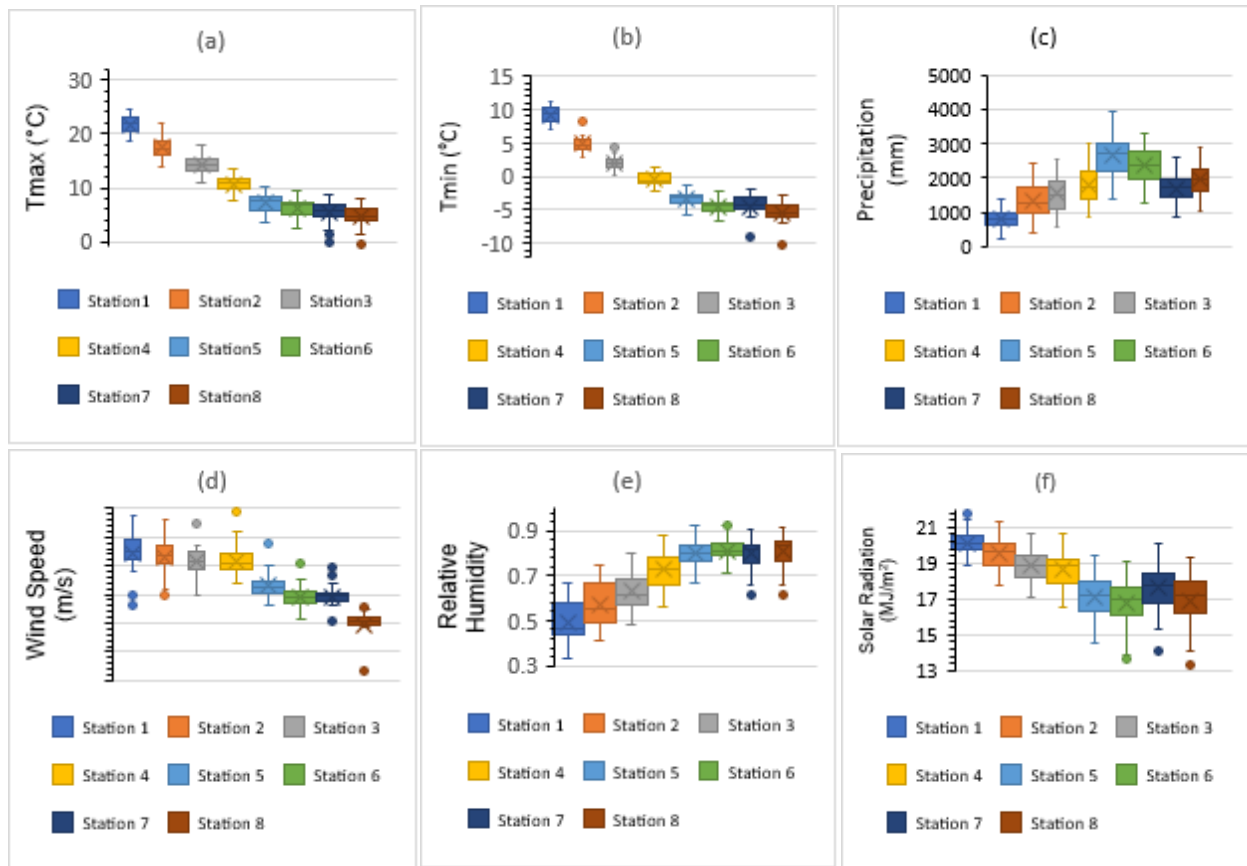


Figure 2. Average annual Streamflow.



**Figure 3.** Baseline climatic analysis (a) Tmax (b) Tmin (c) Precipitation (d) Wind speed baseline climatic analysis (e) Relative humidity (f) Solar radiation.

### 3.1.6 Solar Radiation

The solar radiation in the Kunhar River basin followed a pattern similar to the temperature. The highest average annual solar radiation was 20.14 MJ/m<sup>2</sup> at Station 1 and the lowest was 16.7 MJ/m<sup>2</sup> at Station 6. The average annual solar radiation at all eight stations is given in Figure 3(f).

## 3.2 Climatic indices

Results of RCLimDex were divided into three sections; hot, cold, and precipitation extremes.

### 3.2.1 Hot Extremes (SU25, TXx, TNx, TX90p, TN90p, and WSDI)

Six indices of hot extremes were analyzed on an annual basis through the RCLimDex tool at eight different stations across the Kunhar River basin. Spatial variations in the hot extreme indices were determined through the IDW command of ArcGIS. Summer days (SU25) increased prominently at the low elevated stations only. Summer days increased up to 1.7 days per year. However, there was no meaningful change at high elevated stations. Monthly maximum value of daily maximum temperature (TXx) did not show any meaningful change at the downstream stations, but the upstream stations showed negative trends. TXx decreased up to -0.1°C/year, the negative sign showing a decrease in trend. Monthly maximum value of daily minimum temperature (TNx) increased almost in the entire basin, but the noteworthy increase was recorded only at the low elevated stations. Warm nights (TN90p), Warm days (TN90p), and Warm spell duration indicator (WSDI) were increased almost in the entire basin, but the downstream stations were more affected. Absolute values of the hot extreme indices for all eight stations were given in Table 3. The spatial variation in the hot extreme indices showed in Figure 4.

### 3.2.2 Cold Extremes (FD0, TX10p, TN10p, TNn, TXn, and CSDI)

Six indices of the cold extremes were investigated at eight different stations in the Kunhar River basin. Frost days (FD0) have decreased noticeably in the lower and central parts of the basin, the maximum decrease was observed at the tail with the rate of 1.6 days/year. However, at the head of the basin, FD0 showed a marginal increase in trends. The monthly minimum value of daily maximum temperature (TXn) and monthly minimum value of daily minimum temperature (TNn) showed negative trends at the tail while the central and head of the basin showed positive trends. TXn varied from -0.53°C to 0.80°C per year while TNn varied from -0.60°C to 0.45°C per year. Cool nights (TN10p) and cool days (TX10p) showed positive trends in the lower part of the basin, however, they showed negative trends at high elevated stations. Cold spell duration indicator (CSDI) showed lesser cold spells at tail and more at the head in the basin. Spatial variations of the cold extreme indices are shown in Figure 5.

### 3.2.3 Precipitation Extremes (Rx5day, SDII, R10mm, R50mm, CDD, CWD, R95p, R99p, and Prcptot)

Max 5-day precipitation amount (Rx5day) and simple daily intensity index (SDII) showed a negative trend in almost the entire basin except for a couple of stations upstream. Rx5day decreased up to -1.8 mm per year. The number of days above 10 mm (R10) and above 50 mm (R50) represents the intensity of precipitation event. The decrease in the precipitation intensity (R10 and R50) was observed especially at the low elevated stations. Consecutive dry days (CDD) and consecutive wet days (CWD) represent the frequency of the precipitation. A positive trend was detected for CDD in almost the entire basin and the positive trend for CWD was observed especially in high elevated areas. Very wet days (R95p) and extremely wet days (R99p) were investigated to check the extreme events of precipitation. Both indices (R95p and R99p) showed a decrease in the trend of the extreme events of



precipitation almost in the entire basin. Prcptot gives us the idea of the total amount of precipitation received per year. Overall, the total amount of precipitation decreased especially at the tail of the

basin but at the head, it increased. Changes in precipitation extremes per year are given in Table 3. Furthermore, the spatial variation in the precipitation extremes is shown in Figure 6.

**Table 3.** The hot, cold and precipitation indices in the Kunhar basin.

Stations	Station 1	Station 2	Station 3	Station 4	Station 5	Station 6	Station 7	Station 8
<b>Indices</b>	<b>Hot Extremes</b>							
SU25	0.81	1.73	0.99	-0.14	-0.05	-0.03	-0.01	0.00
TR20	0.37	0.05	0.00	0.00	0.00	0.00	0.00	0.00
TXx	0.03	0.02	0.00	-0.10	-0.11	-0.05	-0.09	-0.07
TNx	0.04	0.07	0.03	0.03	0.01	0.00	0.01	0.02
TN90p	0.59	1.05	0.67	0.36	0.11	-0.02	0.13	0.09
TX90p	0.66	1.28	0.85	0.50	0.05	0.03	-0.04	0.00
WSDI	0.86	1.84	0.74	0.42	0.32	0.21	0.40	0.37
<b>Indices</b>	<b>Cold Extremes</b>							
FD0	-1.31	-1.58	-1.29	-0.92	-0.12	-0.26	0.58	0.31
TXn	-0.50	-0.53	-0.41	-0.42	0.25	0.35	0.99	0.81
TNn	-0.77	-0.60	-0.45	-0.47	0.02	0.11	0.55	0.45
TN10p	0.20	0.25	0.06	0.10	-0.05	-0.10	-0.07	-0.12
TX10p	0.08	0.09	0.04	0.02	-0.05	-0.05	-0.10	-0.09
CSDI	-0.90	-0.55	-0.39	-0.29	0.04	0.04	0.63	0.56
<b>Indices</b>	<b>Precipitation Extremes</b>							
Rx5day	0.04	-1.76	-2.14	-0.42	0.19	-0.11	-0.19	0.04
SDII	-0.04	-0.08	-0.08	-0.05	0.01	0.01	-0.01	0.01
R10	-0.08	-0.76	-0.80	-0.47	-0.05	0.19	0.06	0.28
R50	-0.02	-0.28	-0.08	-0.05	-0.01	0.01	-0.01	0.02
CDD	-0.27	0.42	0.42	0.41	0.17	0.19	0.04	-0.07
CWD	0.26	-0.09	-0.05	0.05	-0.04	0.14	-0.06	0.05
R95p	-2.31	-7.85	-8.97	-7.38	-2.18	-0.03	-1.24	2.36
R99p	0.12	-2.95	-3.69	-2.10	-1.04	0.28	-0.16	1.50
Prcptot	-2.69	-23.58	-26.53	-16.00	-2.13	2.20	0.44	6.53

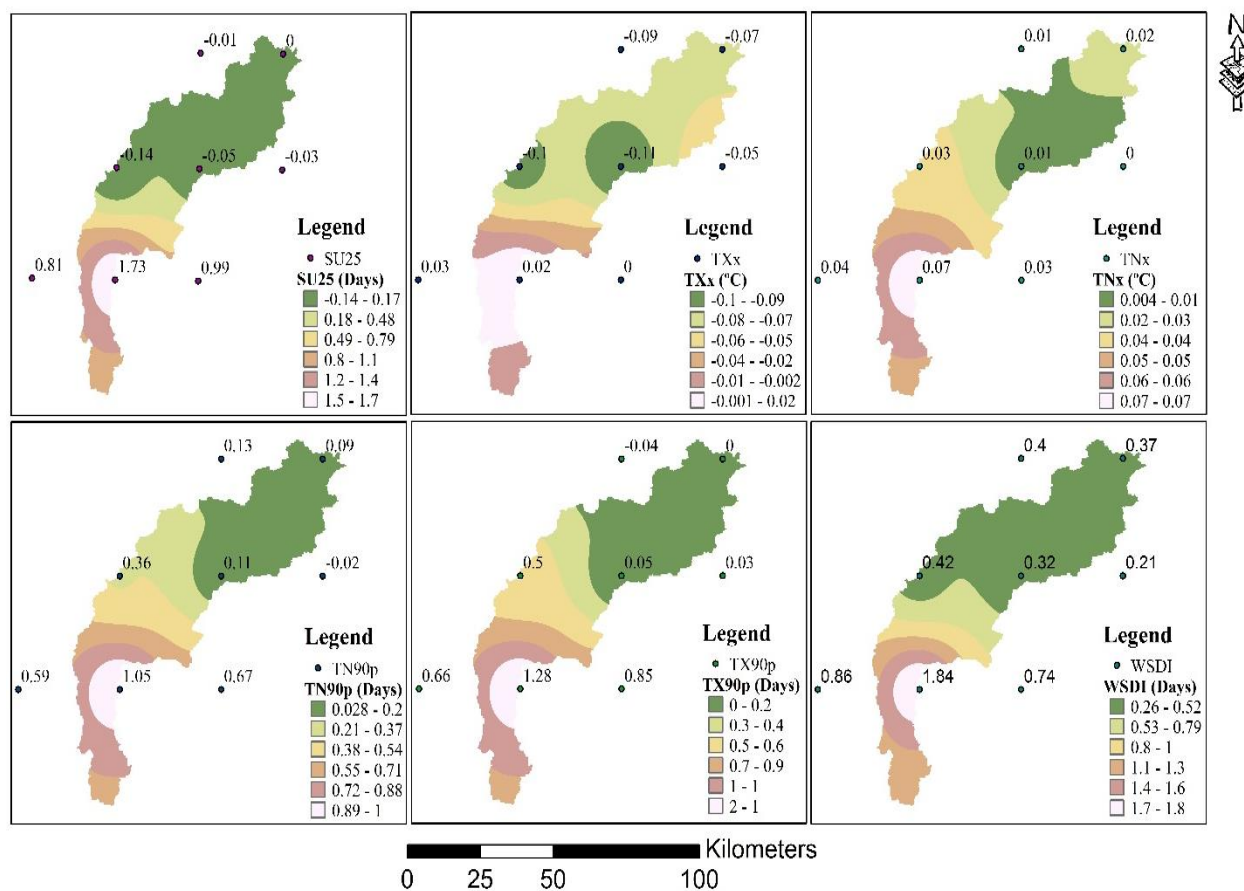


**Figure 4.** Hot extreme indices of climatic parameters in the Kunhar basin.

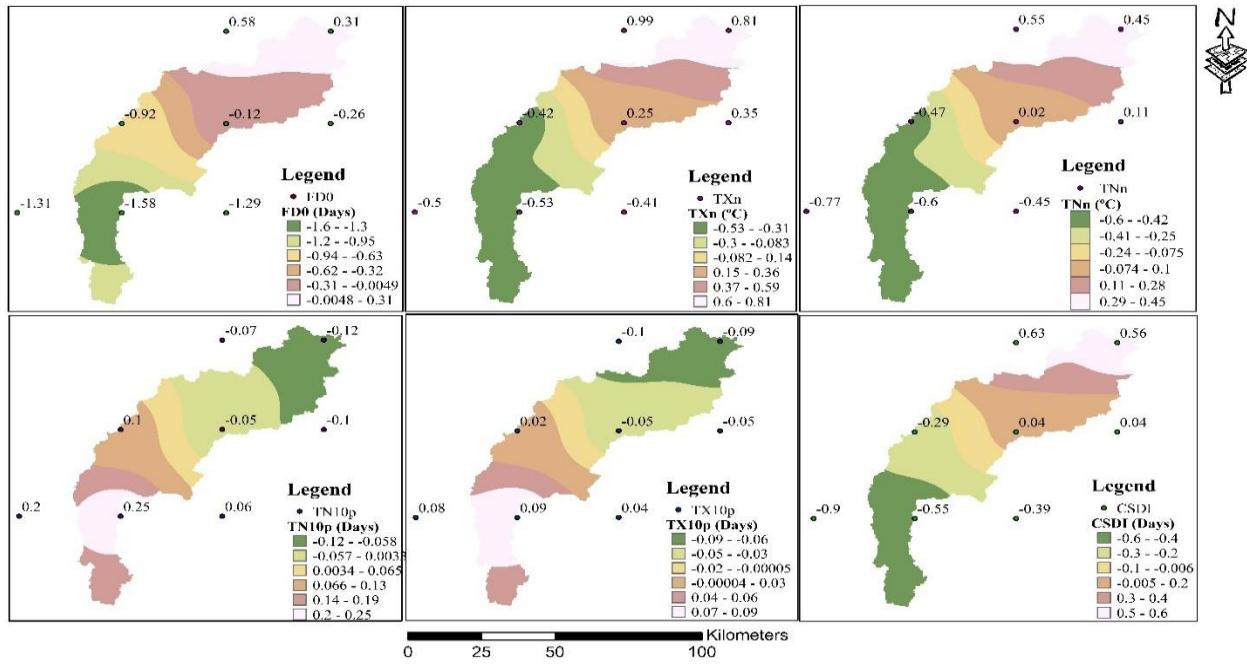


Figure 5. Cold extreme indices of climatic parameters in the Kunhar basin.

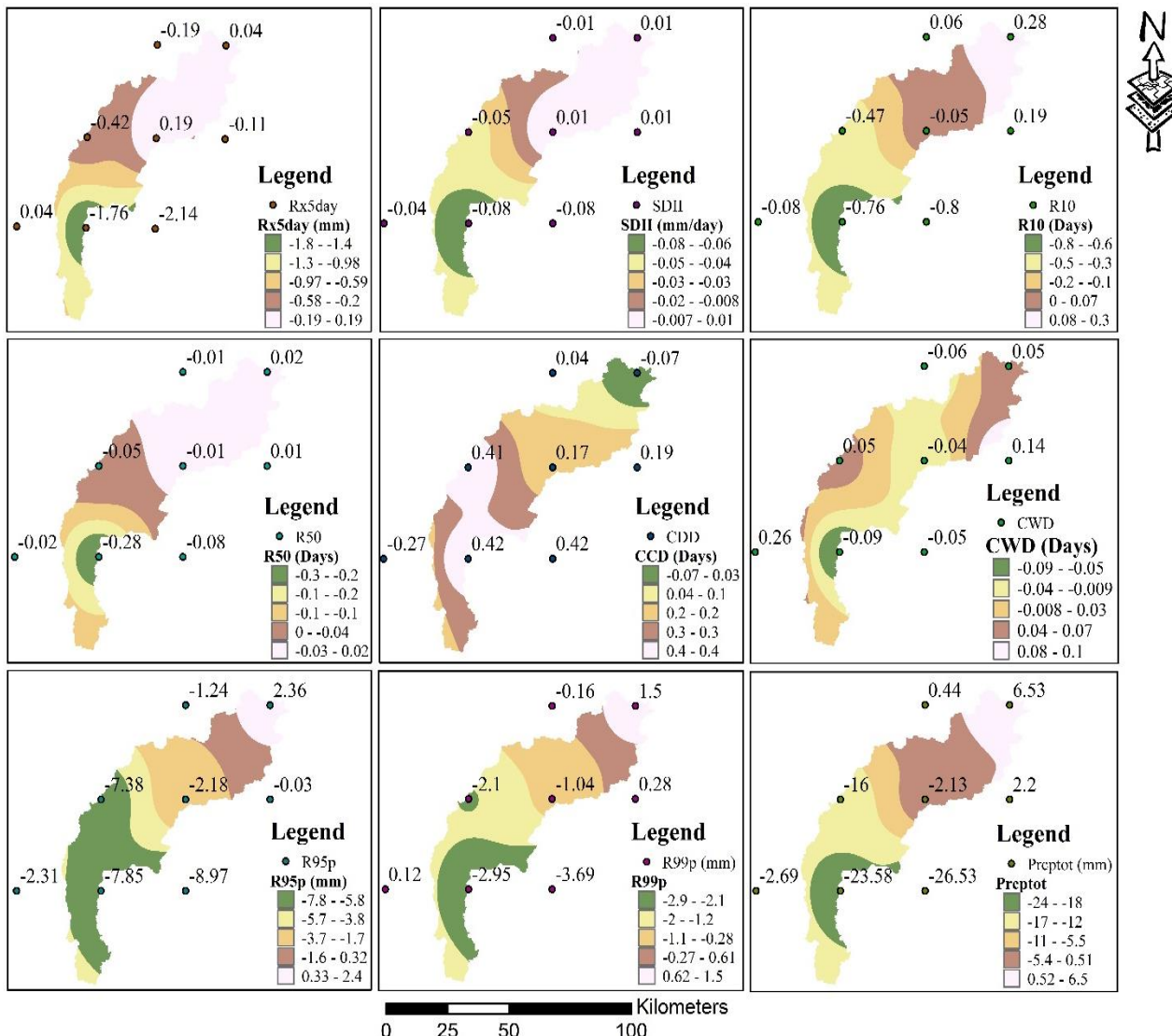


Figure 6. Precipitation extreme indices of climatic parameters in the Kunhar basin.

### 3.3 Trend Analysis

The Mann Kendall test was used to analyze the trends of hydro-climatic parameters. Six parameters of climate (Tmax, Tmin, precipitation, wind speed, relative humidity, and solar radiation) at eight climatic stations and two stations streamflow were investigated in this study.

#### 3.3.1 Hydrological Trend Analysis

The average annual runoff of the Kunhar River was decreasing slightly at Ghari Habibullah with weak significance. However, almost no trend was observed at Naran station. On an annual basis, streamflow showed negative trends. However, the seasonal trends showed mix trends in the Kunhar River basin. Seasonal runoff showed a significant increasing trend at Ghari Habibullah station in the spring season. An increase in streamflow of  $0.415 \text{ m}^3\text{s}^{-1}$  was detected at Ghari-Habibullah in the spring season. Runoff decreased significantly in the summer season at both Naran and Ghari Habibullah stations. The decrease in the streamflow was  $0.437 \text{ m}^3\text{s}^{-1}$ /season of summer at Naran station and  $1.102 \text{ m}^3\text{s}^{-1}$  per summer season at Ghari Habibullah. In the autumn season, the runoff decreased significantly only at the Naran station at a rate of  $0.142 \text{ m}^3\text{s}^{-1}$  per season. There was almost no change in the streamflow in the winter season. The slope (Q) and significance level (Z value) of the streamflow are given at primary and secondary axis respectively as shown in Figure 7.

#### 3.3.2 Climatic Trend Analysis

The maximum temperature increased significantly, especially at downstream stations. The highest increasing slope of  $0.137^\circ\text{C}/\text{year}$  was recorded at Station 2. However, it was also noticed that Tmax decreased at a couple of stations towards the upstream side, with low significance. Trends and significance of maximum temperature (Tmax) are graphically represented in Figure 8(a) where the slope (Q) is given at the primary axis and Z value at the secondary axis. Minimum temperature (Tmin), also showed similar trends at the tail of the basin with even higher significance than Tmax. The highest increasing trend was identified at  $0.087^\circ\text{C}/\text{year}$  at Station 1. However, stations at the head of the basin showed no trends as seen in Figure 8(b). Precipitation decreased significantly at the tail but had no change at the higher elevated stations as shown in Figure 8(c). The maximum decreasing trend in the precipitation of  $2.54 \text{ mm}/\text{year}$  was observed at Station 3.

Wind speed decreased over the entire basin, but a couple of the stations showed weak significance. The highest decreasing trend of  $0.008 \text{ ms}^{-1}/\text{year}$  was noticed at Station 4. Z value and slope (Q) of the wind speed are shown in Figure 8(d). Relative humidity also decreased almost in the entire basin with a strong significance. The greatest decreasing trend was observed at  $0.006 \text{ fractions}/\text{year}$  ( $0.6\%/ \text{year}$ ) at Station 2 with a strong significance. However, stations 7 and 8 were showing no trends. Z value and slope (Q) of the relative humidity are shown in Figure 8(e).

Solar radiation in the Kunhar River basin showed mixed trends. An increase in trends with strong significance was observed at Stations 2, 3, and 4. On the other hand, a decrease in trends was observed at high elevation stations but only Station 8 had strong significance. The maximum increase in the trend of solar radiation was analyzed as  $0.045 \text{ MJ}/\text{m}^2$  at Station 3. In contrast, the maximum decrease in the trend of  $0.040 \text{ MJ}/\text{m}^2$  was obtained at Station 8. The Z value and slope (Q) of the solar radiations are shown in Figure 8(f). A hydroclimatic study conducted earlier for the Mangla Watershed, Pakistan also showed almost similar trends at Naran, Balakot, and Ghari Habibullah stations which lie within the Kunhar River basin [14].

### 3.4 Spatial Variations

For the baseline period (1979-2014), the average annual precipitation in the Kunhar River basin varied from 808 mm to 2219 mm; the highest precipitation is received at the central-eastern part of the basin and the lowest received at the tail (south) of the basin. In general, it decreased from head to tail. The average annual maximum temperature varied from  $4.98^\circ\text{C}$  to  $25.2^\circ\text{C}$ ; temperature increased from top to bottom. A very similar pattern was observed in the case of minimum temperature. The mean annual wind speed varied from  $2.5 \text{ ms}^{-1}$  to  $3.7 \text{ ms}^{-1}$ . The wind speed was higher in most of the stations in the lower half of the basin as compared to the upper part. Moreover, the average annual wind speed was the lowest at the top of the basin. The average annual relative humidity varied from 57% to 81% and the relative humidity (RH) in the upper half part of the basin was approximately 80% however, the lower part of the basin had lower relative humidity. The average annual solar radiation (SR) varied from  $17 \text{ MJm}^{-2}$  to  $20 \text{ MJm}^{-2}$ , increasing from upstream to downstream. The spatial variation in the climatic parameters is shown in Figure 9.

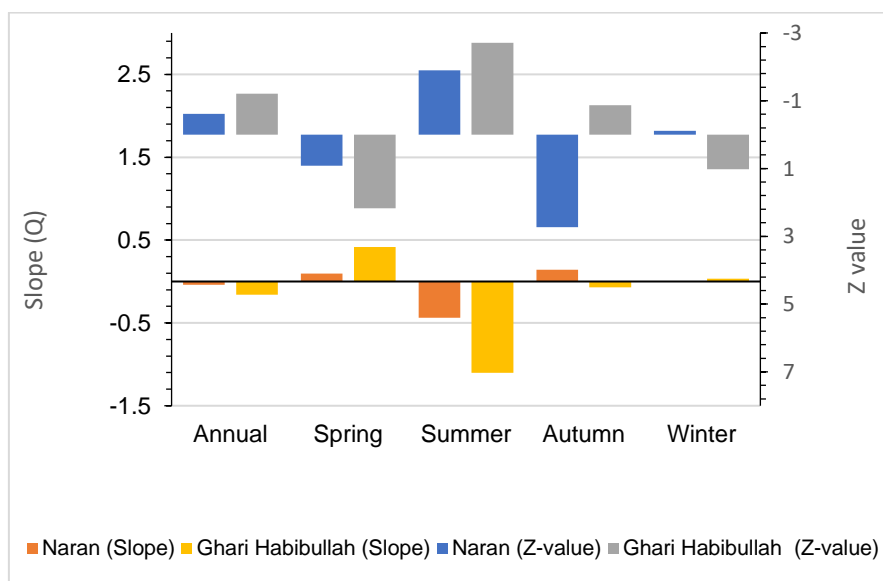


**Figure 7.** Hydrological trend analysis (slope (Q) is given at the primary axis and Z value at the secondary axis).



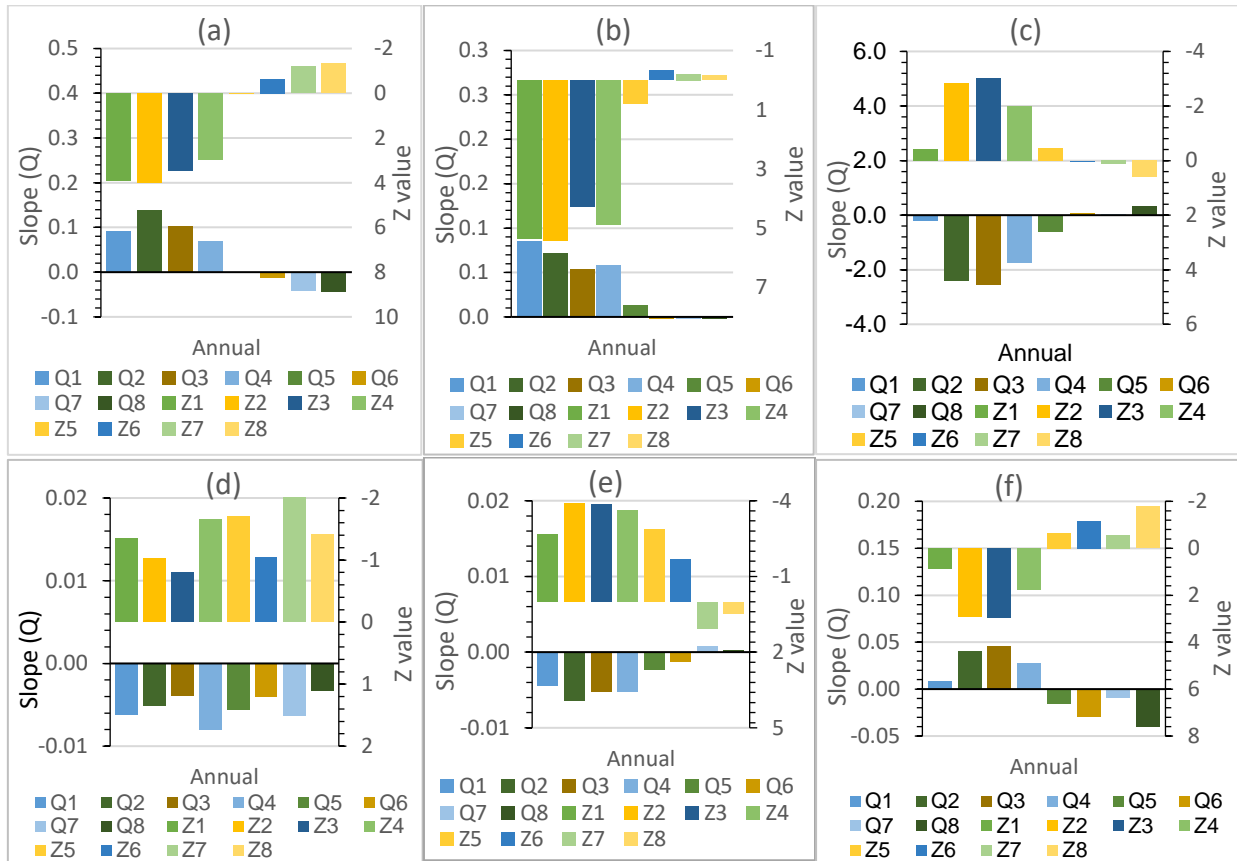


**Figure 8.** Climatic trend analysis (a) Tmax (b) Tmin (c) Precipitation (d) Wind speed (e) Relative Humidity (f) Solar radiation (slope (Q) is given at the primary axis and Z value at the secondary axis).

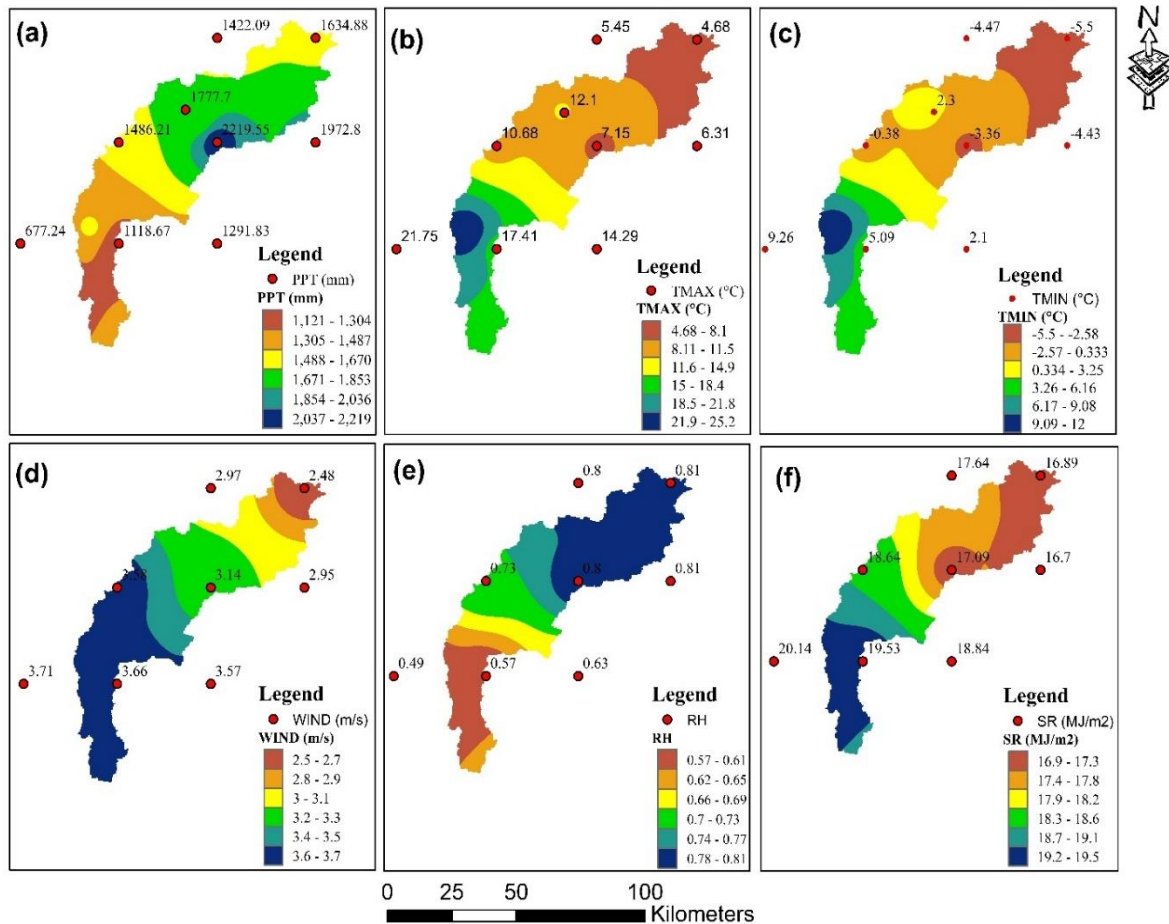


**Figure 9.** Spatial variability of climatic parameters, (a) Tmax (b) Tmin (c) Precipitation (d) Wind speed (e) Relative Humidity (f) Solar radiation.

Higher average annual precipitation, relative humidity, and lower temperature were observed in the upstream side of the basin. Moreover, cold and hot climatic extremes also showed warming trends. Trend analysis through the Mann Kendall test was conducted, which demonstrated that both maximum and minimum temperatures were significantly increased in the downstream side of the basin. Furthermore, an increase in the minimum temperature was higher than the maximum. Precipitation was significantly decreasing at the tail of the basin. The hydrological changes were also evidence of all these climatic changes. The river flow also decreased significantly at the downstream station. Seasonal runoff variation was more pronounced than annual. Changes in climatic parameters especially precipitation and temperature can be helpful for the agriculture, forestry, water resources, and climate change departments. Overall precipitation per annum was decreasing significantly in the lower and middle part of the basin, which can be damaging to the agriculture yield. Because the lower part of the basin had agriculture and forests as a major land use classes and agriculture was one of the basic sources of income for the natives [20]. Baseline climatic extremes and spatiotemporal trends are important as a gateway to check the future climate changes. Moreover, the overall investigation provides valuable information for the policymakers of the climate change department to take decisions, related to Sustainable Development Goals: Clean Water & Sanitation (SDG 6) and Climate Action (SDG 13).

#### 4. Conclusion

Both techniques, RCLimDex and Mann Kendall, showed an increase in temperature and lowering in precipitation, wind speed, and relative humidity trends, especially in the lower half of the basin. Ultimately, river runoff was found to be decreasing annually. However, seasonal variations were observed to be more significant on an annual basis, as the streamflow showed an increase at a rate of 0.415 m<sup>3</sup>/s per spring season. However, at the downstream station, a sharp decrease was observed at a rate of 1.102 m<sup>3</sup>/s per summer season. The sharp seasonal fluctuations are a clear evidence of shifting peak flow; the rate could increase in the upcoming years. Changes in the climatic parameters and indices investigated in this research were found to be more important in the lower part of the basin. The climatic trends are strongly significant and downstream of the basin gets drier and hotter, while wind speed and relative humidity gets lower. These lead to changes in crop water requirements and agriculture yields. An increase in dry spells may also affect the ecosystem of the basin. These changes can make it difficult for policymakers to achieve Clean Water & Sanitation (SDG 6) and Climate Action (SDG 13) in the near future.

#### Acknowledgments

The Surface Water Hydrology Project (SWHP), Pakistan is acknowledged to provide data for the research. The authors would like to acknowledge the Joint Graduate School of Energy and Environment (JGSEE), King Mongkut's University of Technology Thonburi and the Center of Excellence on Energy Technology and Environment (CEE), PERDO, Ministry of Higher Education, Science, Research and Innovation for providing funding to do this research work.

#### References

- [1] Wang, H., Zhang, M., Zhu, H., Dang, X., Yang, Z. and Yin, L. 2012. Hydro-climatic trends in the last 50 years in the lower reach of the Shiyang River basin, NW China, *Catena*, 95, 33-41.
- [2] Gebre, S.L. and Ludwig, F. 2014. Spatial and temporal variation of impacts of climate change on the hydrometeorology of Indus River Basin using RCPs scenarios, *South East Asia, Journal of Earth Science and Climatic Change*, 5(10), 1-7.
- [3] Mahmood, R. and Jia, S. 2017. Spatial and temporal hydro-climatic trends in the transboundary Jhelum River basin, *Journal of Water and Climate Change*, 8(3), 423-440.
- [4] Saifullah, M., Liu, S., Tahir, A.A., Zaman, M., Ahmad, S., Adnan, M., Chen, D., Ashraf, M. and Mehmood, A. 2019. Development of threshold levels and a climate-sensitivity model of the hydrological regime of the high-altitude catchment of the Western Himalayas, Pakistan, *Water*, 11(7), 1454.
- [5] Sharma, A. and Goyal, M.K. 2018. District-level assessment of the ecohydrological resilience to hydroclimatic disturbances and its controlling factors in India, *Journal of Hydrology*, 564, 1048-1057.
- [6] Latif, Y., Yaoming, M. and Yaseen, M. 2016. Spatial analysis of precipitation time series over the Upper Indus Basin, *Theoretical and Applied Climatology*, 131(1-2), 761-775.
- [7] Sahoo, D. and Smith, P.K. 2009. Hydroclimatic trend detection in a rapidly urbanizing semi-arid and coastal river basin, *Journal of Hydrology*, 367(3-4), 217-227.
- [8] Tekleab, S., Mohamed, Y. and Uhlenbrook, S. 2013. Hydro-climatic trends in the Abay/Upper Blue Nile basin, Ethiopia, *Physics and Chemistry of the Earth*, 61-62, 32-42.
- [9] Xu, Z., Liu, Z., Fu, G. and Chen, Y. 2010. Trends of major hydroclimatic variables in the Tarim River basin during the past 50 years, *Journal of Arid Environments*, 74(2), 256-267.
- [10] Archer, D.R. and Fowler H.J. 2004. Spatial and temporal variations in precipitation in the upper Indus basin, global teleconnections, and hydrological implications, *Hydrology and Earth System Sciences*, 8(1), 47-61.
- [11] Khattak, M.S., Babel, M.S. and Sharif, M. 2011. Hydro-meteorological trends in the upper Indus river basin in Pakistan, *Climate Research*, 46, 103-119.
- [12] Rauf, U.A., Rafi, M.S., Ali, I. and Muhammad, U.W. 2016. Temperature trend detection in Upper Indus basin by using Mann-Kendall test, *Advances in Science Technology and Engineering Systems Journal*, 1(4), 5-13.
- [13] Sharif, M., Archer, D.R., Fowler, H.J. and Forsythe, N. 2013. Trends in timing and magnitude of flow in the Upper Indus Basin, *Hydrology and Earth System Sciences*, 17(4), 1503-1516.
- [14] Yaseen, M., Nabi, G., Rehman, H.U. and Latif, M. 2014. Assessment of climate change at spatio-temporal scales and its impact on stream flows in Mangla Watershed, *Pakistan Journal of Engineering and Applied Sciences*, 15, 17-36.
- [15] Mahmood, R. and Jis, S. 2016. Assessment of impacts of climate change on the water resources of the transboundary Jhelum River Basin of Pakistan and India, *Water*, 8(6), 1-18.
- [16] Gautam, M.R., Acharya, K. and Tuladhar, M.K. 2010. Upward trend of streamflow and precipitation in a small, non-snow-fed, mountainous watershed in Nepal, *Journal of Hydrology*, 387(3-4), 304-311.
- [17] Asian Development Bank. 2017. *Climate Change Profile of Pakistan*, 6 ADB Avenue, Mandaluyong City, 1550 Metro Manila, Philippines, Available online: <https://www.adb.org/sites/default/files/publication/357876/climate-change-profile-pakistan.pdf> [Accessed on 27 January 2019].
- [18] Groetzbach, E. 1989. Mountain Tourism in north Pakistan—tourist regions and problems of further development, *Tourism Recreation Research*, 14(2), 69-73.
- [19] Arshad, M.I., Iqbal, M.A. and Shahbaz, M. 2017. Pakistan tourism industry and challenges: a review, *Asia Pacific Journal of Tourism Research*, 23(2), 121-132.

- [20] Moiz, A., Kawasaki, A., Koike, T. and Shrestha, M. 2018. A systematic decision support tool for robust hydropower site selection in poorly gauged basins, *Applied Energy*, 224, 309-321.
- [21] Mahmood, R., Jia, S. and Babel, M. 2016. Potential Impacts of climate change on water resources in the Kunhar River Basin, Pakistan, *Water*, 8(1), 23, 1-24.
- [22] Wang, H., Chen, Y., Chen, Z. and Li, W. 2012. Changes in annual and seasonal temperature extremes in the arid region of China, 1960–2010, *Natural Hazards*, 65(3), 1913-1930.
- [23] Klein, T.A.M.G., Peterson, T.C., Quadir, D.A., Dorji, S., Zou, X., Tang, H., Santhosh, K., Joshi, U.R., Jaswal, A.K., Kolli, R.K., Sikder, A.B., Deshpande, N.R., Revadekar, J.V., Yeleuova, K., Vandasheva, S., Faleyeva, M., Gomboluudev, P., Budhathoki, K.P., Hussain, A., Afzaal, M., Chandrapala, L., Anvar, H., Amanmurad, D., Asanova, V.S., Jones, P.D., New, M.G. and Spektorman, T. 2006. Changes in daily temperature and precipitation extremes in central and South Asia, *Journal of Geophysical Research*, 111(D16), 1-8.
- [24] Manandhar, S., Pandey, V.P. and Kazama, F. 2013. Climate change and adaptation: an integrated framework linking social and physical aspects in poorly-gauged regions, *Climatic Change*, 120(4), 727-739.
- [25] Marofi, S., Sohrabi, M.M., Mohammadi, K., Sabziparvar, A.A. and Abyaneh, H.Z. 2010. Investigation of meteorological extreme events over coastal regions of Iran, *Theoretical and Applied Climatology*, 103(3-4), 401-412.
- [26] Wang, Y., Ding, Z. and Ma, Y. 2019. Spatial and temporal analysis of changes in temperature extremes in the non-monsoon region of China from 1961 to 2016, *Theoretical and Applied Climatology*, 137, 2697–2713.
- [27] Rai, R.K., Upadhyay, A. and Ojha, C.S.P. 2010. Temporal variability of climatic parameters of Yamuna River Basin: spatial analysis of persistence, trend and periodicity, *The Open Hydrology Journal*, 4, 184-210.
- [28] Chen, Y.D., Li, J., Zhang, Q. and Gu, X. 2018. Projected changes in seasonal temperature extremes across China from 2017 to 2100 based on statistical downscaling, *Global and Planetary Change*, 166, 30-40.
- [29] Palaniswami, S. and Muthiah, K. 2018. Change point detection and trend analysis of rainfall and temperature series over the Vellar River basin, *Polish Journal Environmental Studies*, 27(4), 1673-1681.
- [30] Tekleab, S., Mohamed, Y. and Uhlenbrook, S. 2013. Hydro-climatic trends in the Abay/Upper Blue Nile basin, Ethiopia, *Physics and Chemistry of the Earth*, 61-62, 32-42.
- [31] Ahmad, I., Tang, D., Wang, T., Wang, M. and Wagan, B. 2015. Precipitation trends over time using Mann-Kendall and Spearman's rho tests in Swat River Basin, Pakistan, *Advances in Meteorology*, 2015, 1-15.
- [32] Latif, Y., Yaoming, M. and Yaseen, M. 2016. Spatial analysis of precipitation time series over the Upper Indus Basin, *Theoretical and Applied Climatology*, 131(1-2), 761-775.
- [33] Dadic, R., Mott, R., Lehning, M., Carenzo, M., Anderson, B. and Mackintosh, A. 2013. Sensitivity of turbulent fluxes to wind speed over snow surfaces in different climatic settings, *Advances in Water Resources*, 55, 178-189.